

Low angular-dispersion microwave absorption of a metal dual-period nondiffracting hexagonal grating

Matthew J. Lockyear,^{a)} Alastair P. Hibbins, and J. Roy Sambles

Thin Film Photonics Group, School of Physics, University of Exeter, Exeter EX4 4QL, United Kingdom

Christopher R. Lawrence

QinetiQ Ltd, Farnborough, GU14 0LX, United Kingdom

(Received 29 December 2004; accepted 14 March 2005; published online 26 April 2005)

The microwave ($11.3 < \lambda_0 < 16.7$ mm) reflectivity response of a nondiffracting dual-period hexagonal grating is explored. In three directions at 60° to each other, the aluminum grating has a repeat period of 7.2 mm in which are three equally spaced grooves, one being slightly shallower than the other two. This dual-period (λ_g and $\lambda_g/3$) structure exhibits strong microwave absorption at several different frequencies. In addition, some of the absorptions are almost completely independent of the angle of incidence and polarization of the microwave radiation.

© 2005 American Institute of Physics. [DOI: 10.1063/1.1921345]

The coupling of incident radiation to the fundamental electromagnetic charge density oscillation or surface plasmon polariton (SPP) at a metal-dielectric interface has attracted much scientific interest since the initial observation of Wood, 1902.¹ The SPP on a planar interface is nonradiative as the dispersion of the mode exists beyond the light cone. The introduction of a periodic surface such as a diffraction grating not only provides the extra momentum required by the incident radiation to couple to these modes (in integer multiples of the grating wave vector k_g) but also perturbs the mode dispersion, splitting it into a series of bands.

Previous studies have shown that short-period deep metal gratings can support flat-banded standing wave SPP modes localized within the grating grooves.² These self-coupled SPPs have also been associated with high field enhancement³ within the grooves. More recently, theoretical work by Tan *et al.*⁴ has shown that it is possible to couple to an infinite set of flat-banded SPP modes by employing an alternative profile, that of an originally deep sinusoid convolved with a slightly shallower oscillation of longer period described by

$$z = A_1 \sin\left(\frac{2\pi}{l}x\right) + A_n \sin\left(\frac{2\pi}{nl}x + \alpha_n\right), \quad (1)$$

where n is an integer greater than 1. The first term of Eq. (1) is the principal component of the grating with an amplitude of A_1 and a period of l , and predominantly defines the mode dispersion. The secondary longer period of amplitude A_n ($< A_1$) and period nl introduces a Brillouin zone boundary at $2\pi/nl$, folding the dispersion back into the light cone and allowing radiative coupling. Similar coupling has been observed experimentally⁵ using a dual-period square-wave profile in the microwave regime. Further, the characteristic strong resonant absorption associated with the flat-banded mode supported by the dual-period profile has been combined with the ability of crossed gratings to act as polarization-independent selective absorbers by the present authors.⁶ A polarization-independent and largely incident-angle-independent response was obtained from a 90° crossed

and zero-ordered grating, which was an extremely efficient selective absorber of incident radiation. As an extension to this work and to improve the angle-independent nature of the metallic absorbing surface, we present here an azimuth-angle-dependent reflectivity study of a 60° dual-period zero-order hexagonal grating in the microwave regime.

The grating profile of two deep (2.19 mm) and one slightly shallower (1.89 mm) evenly spaced 0.8 mm wide grooves per repeat period of $\lambda_g = 7.2$ mm (producing to first order a deep grating period of $\lambda_g/3$ superimposed by a slightly shallower grating period of λ_g with an aspect ratio of 2:1) was milled in three orientations at 60° with respect to each other into the surface of a circular aluminum alloy plate of radius of 410 mm and thickness of 20 mm. The angle of incidence θ and azimuth angle φ are shown in Fig. 1 together with the reciprocal lattice vectors for this structure. For simplicity, we define $\varphi = 0^\circ$ when one of the grating wave vectors lies in the incident plane.

The combination of hexagonal and dual-period symmetry gives rise to several possible symmetry configurations.

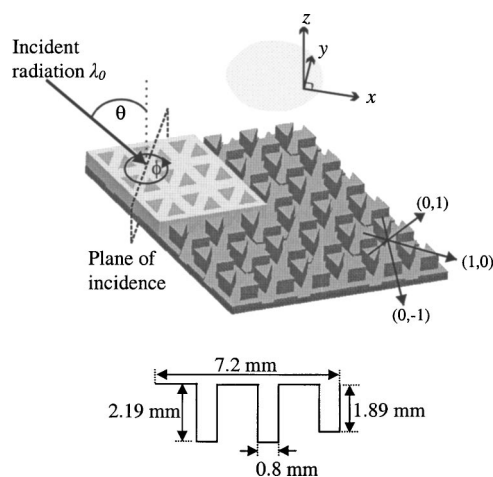


FIG. 1. The unit cell (light region) and coordinate system illustrating the angle of incidence θ , azimuth angle φ , and plane of incidence together with the reciprocal lattice vectors. Primitive lattice vectors are omitted for clarity. Also shown is a schematic representation of a single dual-period grating profile.

^{a)}Electronic mail: m.j.lockyear@exeter.ac.uk

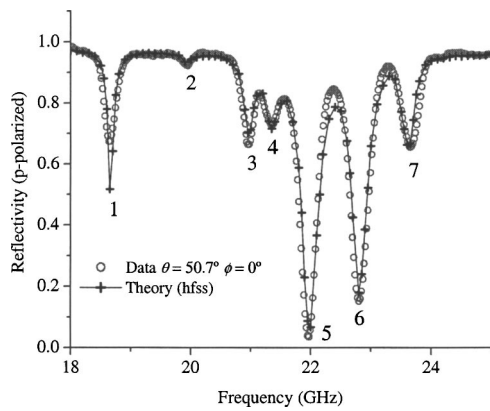


FIG. 2. p -polarized reflectivity data obtained for $\theta=50.7^\circ$, $\varphi=0^\circ$ clearly showing seven resonances as reflectivity minima. The modeled response of the structure (solid line) is obtained using a FEM modeling code.

For the purpose of this study we restrict ourselves to consider the geometry for which a shallow groove from each of the three grating profiles crosses at a single point. Resonant modes may be observed as minima in the angle-dependent reflectivity with the resonance width and depth being dependent upon the loss channels available, with optimum coupling occurring when the nonradiative losses and radiative losses are equal.⁷ The grating under study is nondiffracting over the selected frequency and incident angle ranges, and hence radiative decay through propagating diffracted orders is not an available loss channel. Energy dissipation via Joule heating of the substrate is also low since metals behave as near perfect conductors at microwave frequencies. Hence, to readily observe the resonant modes in reflectivity, the grating grooves are filled with petroleum wax ($\epsilon_d=2.16+0.02i$), which is slightly absorbing at these frequencies. A collimated beam of microwave radiation is directed onto the sample via a spherical mirror. A second mirror is positioned to collect the specularly reflected beam and focus it into the detector. The sample is mounted upon a rotating turntable, providing data for $0 \leq \varphi \leq 360^\circ$ at fixed values of θ , with the signal normalized to the reflectivity of a flat plate of the same material and surface plane dimensions as the substrate. Both the source antenna and detector may be set to pass either

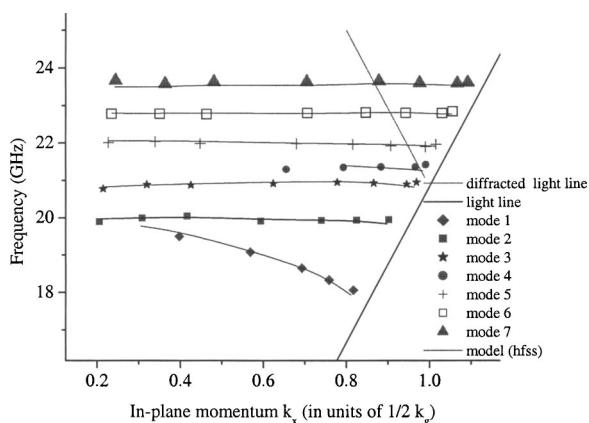
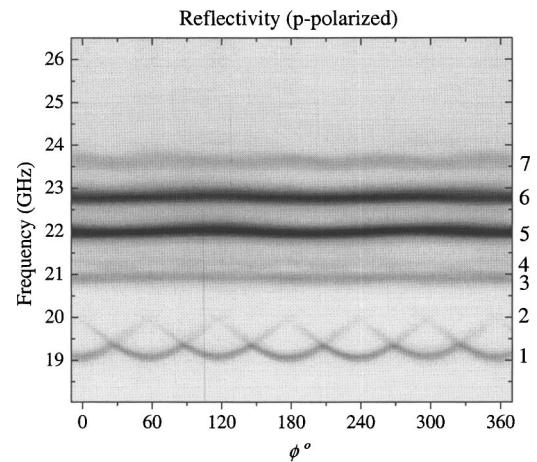
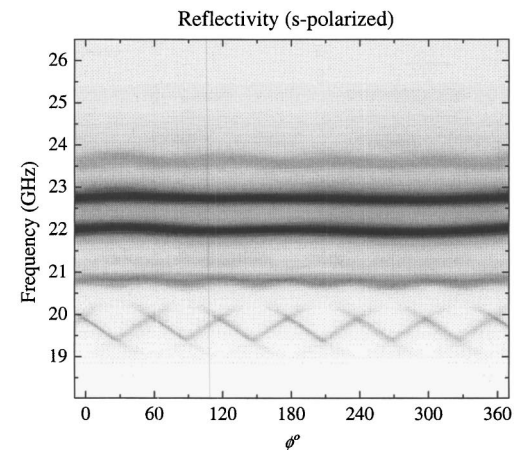


FIG. 3. The experimental and modeled dispersion curves of modes 1 through 7 (1 being the lowest-energy mode and 7 being the highest) at $\varphi=0^\circ$. The position in frequency of each mode in the range $12^\circ < \theta < 75^\circ$ is plotted against the associated in-plane momentum $k_x=(2\pi f/c)\sin\theta$, where f is the resonant frequency and c is the speed of light. Also shown is the light line and the (1,0) diffracted light line.



(a)



(b)

FIG. 4. (a) p -polarized and (b) s -polarized reflectivity data as a function of both frequency and azimuth angle at a fixed polar angle of 38° . Light regions correspond to strong reflection, while dark regions correspond to absorption.

p -polarized (transverse magnetic) or s -polarized (transverse electric) radiation, allowing reflectivity measurements of R_{pp} , R_{ps} , R_{sp} , and R_{ss} (the subscripts refer to the source and detector polarizations, respectively). A full description of the experimental setup may be found in Ref. 8.

Figure 2 shows the p -polarized frequency-dependent reflectivity data for $\theta=50.7^\circ$, $\varphi=0^\circ$ together with the modeled response of the structure obtained from a finite element method (FEM) model,⁹ which divides the entire problem space into a large number of smaller elements (tetrahedra) and solves Maxwell's equations at strategic points within each element numerically, thus providing a full wave solution. Good agreement is obtained between the model and data even though the model assumes a perfect plane wave (the experimental incident angle spread is approximately 1°)⁸ and treats the sample as infinite in the surface plane. A total of seven resonances are visible over the selected frequency range, with the two main resonances absorbing up to 95% and 85% of the incident radiation, respectively.

In order to identify the dispersion of each mode, resonant frequencies at $\varphi=0^\circ$ over the range $12^\circ < \theta < 75^\circ$ are plotted in Fig. 3 against the associated in-plane momentum $k_x=(2\pi f/c)\sin\theta$, where f is the resonant frequency and c is the speed of light. This plot clearly shows the remarkably nondispersive nature of the six higher frequency resonances

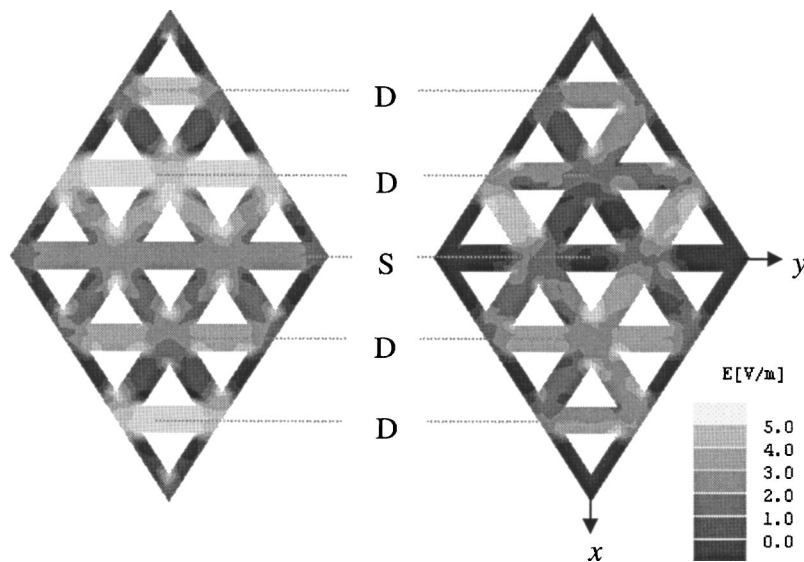


FIG. 5. Time-averaged electric field magnitude at the resonant frequencies of modes 1 and 2 respectively, modeled over a plane parallel to the surface of the grating, at $z = -1.1$ mm (where $z = 0$ is defined as the uppermost surface of the metallic structure in the xy plane). Radiation is incident in the xz plane at an angle of $\theta = 50.7^\circ$ to the normal and is p -polarized. Deep grooves are labeled "D," shallow grooves are labeled "S."

as a function of θ , while the lowest frequency mode is less localized in nature and more dispersive, curving downwards toward k_g at lower frequency. Reflectivities associated with the resonances at 22 and 22.8 GHz are always less than 10% and 22%, respectively, for $\theta < 60^\circ$.

Figure 4 shows (a) p -polarized and (b) s -polarized reflectivity data at $\theta = 38^\circ$, demonstrating the polarization-independent properties of this crossed grating. Dark regions correspond to strong absorption while light regions represent reflection. Modes at 21.0, 22.0, 22.8, and 23.7 GHz are visible and strikingly flat in frequency over the entire range of azimuth angle. It is also clear from the φ -dependent data that the two lowest modes from the dispersion diagram (one of which is nondispersive with θ) exhibit sixfold symmetry imposed by the hexagonal structure. The intersection of modes 1 and 2 (1 being the lowest frequency mode and 7 being the highest) at $\varphi = 30^\circ$ clearly identifies mode 2 as a (0,1) mode, as at $\varphi = 30^\circ$ the (1,0) and (0,1) modes are mirrored about k_x .

To confirm the origins of the lowest two modes, it is useful to evaluate the fields at the resonant frequency of each mode using the finite element code. Figure 5 shows the time-averaged E -field magnitude calculated over a plane parallel to the surface plane of the grating. Regions of high field at the resonant frequency of mode 1 are shown to be confined predominantly to the second deep groove, and display a periodicity of twice the grating pitch in the (1,0) direction only. At the resonant frequency of mode 2, this periodicity is repeated in the (0,1) direction, with regions of high field once again confined to the second deep groove; however, some degree of excitation in the remaining two grating directions is evident.

It is perhaps easiest to consider the hexagonal grating as three single dual-period profiles with associated grating vectors in the (1,0), (0,1) and (1,-1) directions. Each of the three profiles supports a mode originating from (1,0), (0,1) and (1,-1) scatter. These modes are generally more dispersive, and as shown, correspond to modes 1 and 2. Modes 5 and 6 are then the modes arising from higher k_g scattering in the three grating directions. These modes are generally much stronger and nondispersive. Thus, mode 5 is a (2,0) mode,

and mode 6 is a (2,-2), (0,2) mixed mode, since these scattering centres are mirrored about k_x . In a similar manner, 3 and 7 correspond to the modes resulting from (1,1) and (2,2) scatter, respectively.

In this work we have presented an angle-dependent reflectivity study of a dual-period, nondiffracting metal hexagonal grating in the microwave regime. The dual periodicity and sixfold symmetry of the sample results in a structure that supports five remarkably nondispersive SPP modes that are independent of both the direction and polarization of the incident radiation, plus a further two modes that are less localized in nature. Two of the five modes are shown to provide extremely efficient microwave absorption of incident radiation at frequencies that may be predetermined by the physical parameters of the grating. Experimental data show excellent agreement with the theoretically modeled electromagnetic response of the structure.

The authors are grateful for support from the Engineering and Physical Sciences Research Council and the provision of a CASE award by QinetiQ (Farnborough) for one of the authors (M.J.L.). This work was carried out as part of Technology Group 09 of the MoD Corporate Research Fund.

¹R. W. Wood, *Philos. Mag.* **4**, 396 (1902).

²J. R. Andrewartha, J. R. Fox, and I. J. Wilson, *Opt. Acta* **26**, 197 (1979); E. Popov, L. Tsonev, and D. Maystre, *Appl. Opt.* **33**, 5214 (1994); F. J. Garcia-Vidal, J. Sanchez-Dehesa, A. Dechlette, E. Bustarret, T. Lopez-Rios, T. Fournier, and B. Pannetier, *J. Lightwave Technol.* **17**, 2191 (1999); W.-C. Tan, T. W. Priest, J. R. Sambles, and N. P. Wanstall, *Phys. Rev. B* **59**, 12661 (1999).

³F. J. Garcia-Vidal and J. B. Pendry, *Phys. Rev. Lett.* **77**, 1163 (1996); A. Wirgin and T. Lopes-Rios, *Opt. Commun.* **48**, 416 (1984).

⁴W.-C. Tan, J. R. Sambles, and T. W. Priest, *Phys. Rev. B* **61**, 13177 (2000).

⁵A. P. Hibbins, J. R. Sambles, and C. R. Lawrence, *Appl. Phys. Lett.* **80**, 13 (2002).

⁶M. J. Lockyear, A. P. Hibbins, J. R. Sambles, and C. R. Lawrence, *Appl. Phys. Lett.* **83**, 806 (2003).

⁷H. Raether, *Surface Plasmons* (Springer, Berlin, 1988).

⁸A. P. Hibbins, J. R. Sambles, and C. R. Lawrence, *Phys. Rev. E* **61**, 5900 (2000).

⁹www.ansoft.com/products/hf/hfss/index.cfm